

Studies of Intramembrane Transport: A Phenomenological Approach

THOMAS G. KAUFMANN and EDWARD F. LEONARD

Columbia University, New York, New York

The intramembrane transport properties of carbohydrates were investigated in cellophane. The experiments performed were the measurement of net volume transfer under a concentration and pressure gradient and the solute transfer due to a concentration difference together with the physical properties of the membrane. The matrix of phenomenological coefficients characteristic to the transport was established after the phase boundary contributions were extricated from the experimental transport data. These thermodynamic coefficients were then interpreted through the Spiegler-Kedem-Katchalsky frictional model.

The analysis of the frictional coefficients clearly indicated the importance of solute-polymer interactions. The magnitude of solute-solvent frictional coefficients in the membrane were compared with the corresponding interactions in free solutions. Their differences were explained in terms of the interaction of the solute with the macromolecular network and were quantitatively expressed by introducing two reduced frictional coefficients. The tortuosity factor was shown to be related to these interactions and not a simple geometric property of the membrane. The temperature dependence of the frictional coefficients was established.

Recognition of the potential applicability of membrane processes to the chemical industries, water demineralization, biological separations, and to artificial human organs has greatly increased in recent years. However, the basic principles of membrane transport are still not well understood. The phrase *membrane transport*, as it will be used subsequently, actually refers to two different but largely inseparable phenomena: the mechanism by which material is transported across a barrier, which will be designated as *intramembrane transport*, and the resistance to mass transfer always associated with fluids contacting any barrier, which will be called the *phase boundary resistance*. This paper presents a study on intramembrane transport. A parallel investigation of phase boundary phenomena is described in a separate paper (14).

A semipermeable membrane is one which permits the passage of one or more, but not necessarily all, constituents of a solution under the influence of the gradients of their chemical potentials. At the present time, there are many theories (1, 2, 9, 11, 22, 25, 26, 35), each supported by at least some experimental evidence, which purport to state the mechanism by which substances pass through a membrane. However, none of those theories is capable of a general characterization of the transport process.

The application of irreversible thermodynamics to intramembrane transport (15) has established a firm theoretical groundwork for intramembrane studies. The theory provides an exact description of the physical process by defining the necessary number of coefficients required to characterize the permeability of a membrane system. Although this is a very important and imperative first step, it still does not give any clues toward the elucidation of the transport mechanism from a structural viewpoint, due to the inherently abstract nature of thermodynamics. The interpretation of the thermodynamic coefficients requires a physical model. A frictional model proposed by Spiegler, Kedem, and Katchalsky (16, 17, 29) was adopted in this investigation. Their treatment is concerned with the balance of thermodynamic and "mechanical" forces during a quasistationary state of

flux in the membrane. The driving forces are represented by the local gradients of chemical potentials, whereas the retarding forces are represented by the frictional interactions between three components (in the case of a binary system): solute, solvent, and the macromolecular network of the membrane. These frictional coefficients afford a means of studying the relative importance of the various interactions inside the membrane, and thus one may hope to gain from them a clearer physical picture of the nature of transport processes.

The main objectives of this study were the phenomenological characterization of the membrane transport, and the determination of the different frictional coefficients for three carbohydrate-water systems at various temperatures. Also, considerable attention was given to the analysis of phase boundary phenomena (14). This was necessary since an often unwarranted simplification introduced in analyzing membrane transport data is the assumption that the only resistance to mass transfer is that offered by the membrane. The resistance to transport in the fluids next to the membrane is an inescapable concomitant of the membrane resistance. It can partially or completely control the rate process and thus mask the properties of the membrane itself. Consequently, in conjunction with the intramembrane study we have established the mechanism of phase boundary mass transfer (14). This enabled us to extricate all the phase boundary contributions from the experimental transport data, and the various transport coefficients discussed next are characteristic to the membrane alone.

Let us now briefly examine the basic postulates of irreversible thermodynamics and how it is applied to membrane transport.

THEORETICAL BACKGROUND

Basic Concepts of Irreversible Thermodynamics

Irreversible thermodynamics provides rigorous equations relating measurable properties of systems in which transport processes are taking place—provided they are not far removed from equilibrium. In brief, the theory says (7):

1. The thermodynamic variables for a nonequilibrium system are the same functions of the local state as the corresponding equilibrium quantities.

Thomas G. Kaufmann is with Esso Research and Engineering Company, Florham Park, New Jersey.

2. The rate of entropy production inside such a system can be expressed as

$$\dot{T} = \sum_i J_i X_i \quad (i = 1, 2 \dots n) \quad (1)$$

where X_i are the generalized thermodynamic forces, and J_i are the fluxes or flows caused by the forces.

3. The flows J_i of Equation (1) are related linearly to the forces X_i by phenomenological relations of the general type

$$J_i = \sum_j L_{ij} X_j \quad (i, j = 1, 2 \dots n) \quad (2)$$

The L_{ij} are called phenomenological coefficients. Transport processes taking place simultaneously may interfere and produce cross phenomena.

4. If the J_i 's and the X_i 's are mutually independent and certain other conditions are satisfied, then the matrix of phenomenological coefficients is symmetric, that is

$$L_{ij} = L_{ji} \quad (3)$$

The equality expressed in Equation (3) is known as the Onsager reciprocal relation. It was derived by Onsager and based on the statistical mechanical concept of microscopic reversibility. Recently, the symmetry of the matrix of coefficients appears to have been established by Sliepcevic (27) through the application of classical thermodynamics. The validity of this derivation is still under discussion.

Application of the Theory to Membranes

The general theory of solute permeable membranes, from the standpoint of irreversible thermodynamics, was first given by Staverman (30, 31) and Kirkwood (18). The results were further expanded and specifically applied by Kedem and Katchalsky (16).

Consider a homogeneous membrane of thickness Δx separating two compartments, each containing a nonelectrolyte and water. Regarding the membrane as a surface of discontinuity, assume the forces $X_1 = \Delta P$ and $X_2 = \Delta c_s$ to be operative between the compartments. The conjugate fluxes can be defined as the total volume flow (15):

$$J_v = \dot{n}_w \bar{V}_w + \dot{n}_s \bar{V}_s \quad (4)$$

and the exchange flow

$$J_D = \frac{1}{\bar{c}_s} \dot{n}_s - \frac{1}{\bar{c}_w} \dot{n}_w \quad (5)$$

where \dot{n}_w and \dot{n}_s are the number of moles of solvent and solute, respectively, passing through the membrane per unit area, and \bar{V}_w and \bar{V}_s are the partial molal volumes. The term \bar{c}_s is defined as

$$\bar{c}_s = \Delta c_s / \ln \frac{c_s^{\text{II}}}{c_s^{\text{I}}} \quad (6)$$

The rate of entropy production for this system is

$$\dot{T} = J_v \Delta P + J_D RT \Delta c_s \quad (7)$$

The fluxes now can be written as linear, homogeneous functions of the forces

$$J_v = L_p \Delta P + L_{pD} RT \Delta c_s \quad (8)$$

and

$$J_D = L_{Dp} \Delta P + L_D RT \Delta c_s \quad (9)$$

also

$$L_{pD} = L_{Dp} \quad (10)$$

Equation (10) follows from the Onsager reciprocal relation. Equations (8) and (9) show the interdependence of the flows. In the absence of a pressure gradient, Δc_s still produces a volume flow which is usually referred to as the osmotic flow. On the other hand, a pressure difference, besides a total volume flow, also induces a relative difference in the flow of solute and solvent.

Staverman (30) defined the reflection coefficient σ as the ratio

$$\sigma = - \frac{L_{pD}}{L_p} \quad (11)$$

For a nonselective membrane, $\sigma = 0$ and for an ideally semipermeable one, $\sigma = 1$.

Frictional Model

The general phenomenological description of membrane processes yields only very little information about the mechanism of transport on a molecular level. It is necessary to give an interpretation to the thermodynamic coefficients in terms of a given model to obtain this information. The first work of this type concerning membranes was done by Spiegler (29). He applied a frictional model to ion exchange membranes. Spiegler's treatment was extended by Kedem and Katchalsky (16).

The system to be considered is a homogeneous phase of thickness Δx . The local flows of solute and water are designated by J_s and J_w , respectively, and the driving forces are the local gradients of the chemical potentials X_s and X_w . It is assumed that during a quasistationary flux through the membrane, the thermodynamic driving forces X_i are counterbalanced by the frictional forces F_{ij} between various entities. These frictional forces are in turn proportional to the relative velocities v_{ij} of the species involved. The frictional coefficients f_{ij} are defined by this last relation:

$$F_{ij} = -f_{ij} (v_i - v_j) \quad (12)$$

By choosing the membrane as a frame of reference, $v_m = 0$, one can write

$$X_s = -F_{sw} - F_{sm} = f_{sw} (v_s - v_w) + f_{sm} v_s \quad (13)$$

$$X_w = -F_{ws} - F_{wm} = f_{ws} (v_w - v_s) + f_{wm} v_w \quad (14)$$

where F_{sw} , F_{sm} , and F_{wm} represent the frictional forces between solute and water, between solute and the membrane matrix, and between water and the membrane matrix, respectively. At this point, one should be more explicit as to what these frictional coefficients mean. For molecules, the macroscopic concept of friction is not very meaningful. As pointed out by Spiegler, the hindrance of the straight line motion of a molecule has to be envisioned as a multitude of collisions with other particles and with the membrane matrix. These collisions force the molecule into a tortuous path and thus increase the time required for it to pass through the membrane. In essence, therefore, one can consider the effect of collision similar to that of friction since both result in reducing the apparent velocity of a particle. Expressing now the fluxes across the membranes in terms of the local velocities, Equations (13) and (14) can now be integrated (16). In the integration, it is assumed that the chemical potentials of both species are continuous across the boundaries of the membrane and that the frictional coefficients are independent of concentration. Then with the use of Equations (8) and (9), the frictional coefficients can be related to experimentally measured quantities (16):

$$\sigma = 1 - \frac{\omega \bar{V}_s}{L_p} - \frac{K_D f_{sw}}{\phi_w (f_{sw} + f_{sm})} \quad (15)$$

$$\omega = \frac{K_D}{\Delta x (f_{sw} + f_{sm})} \quad (16)$$

$$L_p = \frac{\phi_w}{\Delta x \left[\frac{f_{wm}}{\bar{V}_w} + \bar{c}_s (1 - \sigma) f_{sm} \right]} \quad (17)$$

where the term ω is defined as the solute permeability coefficient at zero volume flow:

$$\omega = \left(\frac{\dot{n}_s}{RT \Delta c_s} \right)_{J_v=0} \quad (18)$$

K_D is the distribution coefficient of solute between the membrane and solution, and ϕ_w is the volume fraction of water in the membrane. The experiments necessary for evaluating these coefficients are described next.

EXPERIMENTAL PHASE AND PRELIMINARY DATA ANALYSIS

The experimental phase of this investigation consisted of determining three sets of force-flux relationships and evaluating various pertinent membrane characteristics. Three solutes—glucose, sucrose, and raffinose—were studied at 27°, 37°, and 47°C. Actually, the following measurements were made; solute transfer under concentration gradient; volume flow due to pressure gradient; volume flow due to concentration gradient; membrane thickness; the solute distribution between the membrane and the surrounding solution, and water content and density of membrane.

The membrane used was a DuPont cellophane. Cellophane, a regenerated cellulose, is regarded as a linear chain of anhydrous betagluco-side units which are linked together by the fourth oxygen atom (10). The films have a low degree of crystallinity and mainly consist of amorphous regions where the chains have no definite pattern of orientation. Swelling may occur when another substance enters the macromolecular network of the film. The swelling phenomenon is primarily attributed to the hydrogen bonding of water molecules to the available hydroxyl groups in the membrane matrix. A preliminary study showed that membranes taken even from the same roll varied in their permeability characteristics. Since it was absolutely essential that in all experiments they should exhibit the same behavior, the following procedure was adopted. The sucrose permeability of a membrane at 37°C. and 200 rev./min. was set up as a standard. A new membrane was accepted or rejected according to this standard.

The apparatus used in the transport studies was a batch dialyzer designed specially to withstand a few atmospheres. It consisted of two almost identical chambers 2.94 in. in diameter and about 2.44 in. in length. Each chamber was equipped with a heater, thermistor probe, calibrated pipette, plunger, and stirrer. The volume of the left side compartment was 236 ml., that of the right 244.5 ml. The chambers were made of Lexan and stainless steel. Each contained an internally mounted four-blade paddle type of stirrer which was driven from the outside by a magnetic coupling. In this way leakage was eliminated as no shaft passed through the wall of the compartments. The driving magnet was joined to a motor which could be moved along rails to interlock with the magnetic housing in the chamber. Two $\frac{1}{50}$ hp. variable-speed Bodine motors equipped with Heller Thyatron Motor controllers were used. The temperature sensing element was a thermistor probe and the solutions were controlled to 0.01°C. with a Thernistemp temperature controller. The compartments also contained plungers which were used to compensate for volumes removed in sampling. This was necessary in order to prevent the partial masking of the membrane by entrained air. A detailed drawing of the right compartment is shown in Figure 1.

The two chambers were brought together by a large knurled lock nut. They had mating flanges, one of them having an O-ring in its face. In order to make the system pressure tight, all parts penetrating the cells were sealed with O-rings. The sampling was done through calibrated pipettes which were attached to the chambers by Swagelock fittings. The stirrer speed was measured with a Number 1531-A, General Radio Company Strobotac.

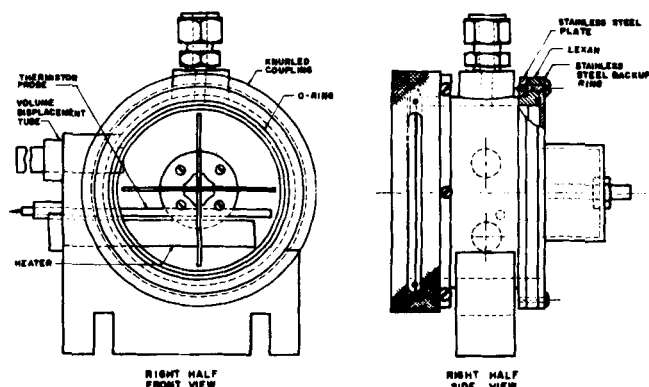


Fig. 1. Right side of batch dialyzer.

Measurement of Solute Permeation Rates

Neither the direct measurement of the phenomenological coefficient L_D nor that of the solute permeability coefficient at zero volume flow ω is convenient. Therefore the so-called dialysis coefficient K_v was determined and then related mathematically to ω and L_D ; K_v is defined by the equation

$$\frac{d(V^I c^I)}{dt} = K_v A (c^{II} - c^I) \quad (19)$$

where c is the solute concentration, A is the membrane area, and the superscripts refer to the compartments. One side of the dialyzer was charged with an approximately 0.1 molar solution and the other one with 0.005 molar. The runs were made at various stirrer speeds ranging from 40 to 500 rev./min. Their duration varied between 5 to 7 hr. depending on the solute used. Three 1-ml. samples were withdrawn after the midpoint and at the termination of the run. The plungers were pushed into the body of the chambers to compensate for volume changes due to sampling and transport. In these experiments the membrane was unsupported. The analysis of solutions was performed by an Industrial Instrument Cryoscope (Model CY-1).

In calculating the dialysis coefficient from solute permeation rates, it is necessary to take into account the simultaneous movement of the solvent across the membrane. The analysis presented below will consider all fluxes across the membrane.

The defining equation for the dialysis coefficient K_v is

$$-\frac{dN^{II}}{dt} = \frac{dN^I}{dt} = K_v A (c^{II} - c^I) \quad (20)$$

where the time derivatives refer to the net rate of solute transfer. The total volume transport is given as

$$\frac{dV^{II}}{dt} = -\frac{dV^I}{dt} = L_p D A (c^{II} - c^I) RT \quad (21)$$

A material balance yields

$$\frac{dN^I}{dt} = \frac{d(V^I c^I)}{dt} = V^I \frac{dc^I}{dt} + c^I \frac{dV^I}{dt} \quad (22)$$

$$\frac{dN^{II}}{dt} = \frac{d(V^{II} c^{II})}{dt} = V^{II} \frac{dc^{II}}{dt} + c^{II} \frac{dV^{II}}{dt} \quad (23)$$

Combining (20), (21), (22), and (23), we find

$$-\frac{d(c^{II} - c^I)}{dt} = K_v A (c^{II} - c^I) (1/V^{II} + 1/V^I) + RT L_p D A (c^{II} - c^I) (c^{II}/V^{II} + c^I/V^I) \quad (24)$$

The integration of Equation (24) is easily carried out if it can be shown that the terms $(1/V^{II} + 1/V^I)$ and $(c^{II}/V^{II} + c^I/V^I)$ are approximately constant for the duration of a run. The maximum change in both was about 1% in this work. Their average values was substituted in Equation (24). Integrating between $t=0$ and $t=\tau$ yields

$$\ln \frac{(c^{II} - c^I)_0}{(c^{II} - c^I)_\tau} = K_v A (1/V^{II} + 1/V^I) \tau + RT L_p D A (c^I/V^I + c^{II}/V^{II}) \tau \quad (25)$$

Equation (25) was used to calculate K_v from the experimental quantities. Two determinations were made at each stirrer speed. The results indicated that K_v is strongly dependent on the agitation rate.

Measurement of the Filtration Coefficient L_p

At zero concentration difference across the membrane, the volume flow is related to the pressure gradient by the filtration coefficient L_p :

$$J_v = L_p \Delta P \quad (26)$$

Since the membrane is very weak, it had to be supported under pressure; otherwise it would have ruptured. This support was provided by a $\frac{1}{8}$ -in. thick porous stainless steel disk obtained from the Pall Corporation, Glenn Cove, New York. The disk was covered by Whatman No. 541 filter paper in order to avoid scratching of the membrane.

Pressure was applied to one side of the dialyzer while the other side was open to the atmosphere and equipped with a calibrated pipette. By noting the rate of advancement of the meniscus in the pipette, the volume flow was determined. In these runs, the initial solute concentration was the same on both sides of the membrane. Care was taken to remove all entrained air. After the chambers were filled, one of them was slowly pressur-

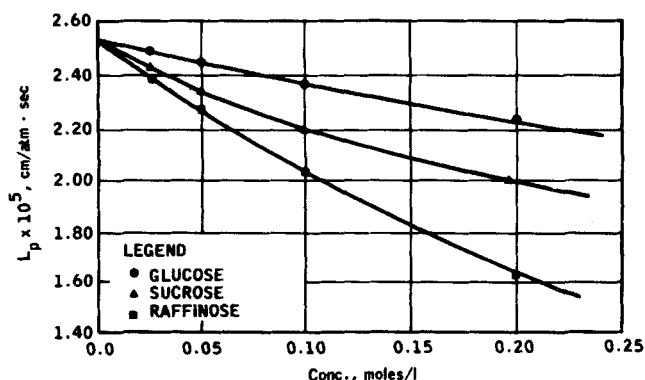


Fig. 2. Dependence of filtration coefficient on solute concentration.

ized. Following this, sufficient time was allowed to obtain a steady state. Usually no more than three or four measurements were taken in order to avoid the buildup of any significant concentration gradient which would invalidate Equation (26). Leakage under pressure presented the greatest problem and it took a considerable effort to make the system leaktight.

In measuring the filtration coefficient L_p , various points had to be clarified before the required data were obtained. The membrane and its support form a resistance in series. Preliminary tests showed that the membrane support has a negligible resistance to volume flow in comparison to the membrane itself. Therefore it was assumed that the measured L_p is not influenced by the presence of the porous plate and filter paper. The effect of pressure on filtration coefficient was investigated for pressure differences ranging from 10 to 180 cm. Hg. The results indicated that in this range L_p is independent of the applied pressure difference. Another point which caused some concern was the influence of solute concentration on volume flow. This effect has received very little attention in the past. For dilute solutions, up to 0.1 M, L_p was thought to be independent of concentration. A careful study for the three systems revealed significant concentration effects even under 0.1 M. The family of curves for the various solutes shown in Figure 2 indicates that L_p is influenced by not only the concentration but by the nature of solute also. Therefore, in calculating the frictional coefficients, one must evaluate L_p at the exact concentration of interest. The filtration coefficient was found to be independent of the stirring rate. This implied that there is no significant boundary-layer resistance to volume flow and the measured L_p refers to the membrane only. During the course of these measurements the membranes were systematically checked to make sure that there was no change in their permeability characteristics due to pressure. The final runs were made under a pressure differential of about 80 cm. Hg at 0.05 M concentration. At any given conditions four replicate runs were made.

The Measurement of the Cross Coefficient L_{pD}

At zero pressure difference the concentration gradient is related to volume flow by the phenomenological coefficient L_{pD} :

$$J_v = L_{pD} RT \Delta c_s \quad (27)$$

The experimental determination of this coefficient caused the greatest difficulties since the magnitudes of volume changes involved are extremely small. One of the main problems was to keep the membrane stationary. The slightest hydrostatic pressure difference caused by unequal liquid levels in the compartments makes the membrane bulge (elastically deform), which in turn masks the volume flow.

First, an attempt was made to calibrate this elastic deformation as a function of pressure difference due to the level changes. Vink (34) has derived an equation which related the volume involved in bulging to the difference in levels in the pipettes. The constant which relates these quantities was evaluated by changing abruptly the liquid level on one side of the dialyzer. It was found that the results were reproducible only to about 10%. Supporting the membrane with thin wires improved the reproducibility but still quite often there were large random deviations. Consequently, this approach was rejected. Next, two perforated aluminum plates were tried as membrane supports. The plates were 0.033 in. thick and the membrane was clamped between them. The surfaces of the plates were ground and then lapped together. Approximately one-quarter of the total area was made available for transport by drilling 391 holes of 0.07 in. diameter in a triangular pattern. The drawback of this approach was that the holes created cylindrical channels of 0.033 in. length in which there was less turbulence than in the main fluid body. Hence,

besides the membrane and boundary-layer resistance one had to take into account this resistance also. Furthermore, there were frequent leakage problems with this setup, and the total volume transport was reduced because of the smaller area. For the above reasons this approach was also rejected.

The method finally adopted was to support the membrane with the porous plate used in the determination of L_p . A very low "standard" pressure was applied from one side to keep the membrane in the same position whenever a volume measurement was made. This pressure was put on only for very short durations in order to avoid any additional volume flow. The runs lasted from 10 to 20 min. At the end a sample was withdrawn and its concentration determined. From the solute permeability coefficient and this concentration the driving force was determined. Stirring was found to be a very important factor in measuring the cross-coefficient L_{pD} . The transfer rates were strongly dependent on the rate of agitation which indicated phase boundary effects. Hence, the measured value of L_{pD} is not a characteristic of the membrane and will be called L_{pD}^* . The correct values were extricated from L_{pD}^* 's in a similar manner to that of the dialysis coefficient (14). The average solute concentration in these runs was the same as in the solute transfer measurements. At each stirrer speed four determinations were made.

Distribution Coefficient

The distribution coefficient relates the concentration of the solute in the sorbent to the concentration of the solute in the external solution. It can be defined as

$$K = \frac{\bar{c}_{\text{sorbent}}}{c_{\text{solution}}} \quad (28)$$

where \bar{c}_{sorbent} refers to moles of solute per unit volume of swollen sorbent and c_{solution} to moles of solute per unit volume of external solution. This definition is in accordance with the one assumed in the thermodynamic analysis, that is, it regards the membrane as a homogeneous phase.

The sorption experiments were carried out in 25-ml. ground glass stoppered flasks. Eight to ten membranes, each having an area of 47 sq. cm., were placed into a flask with 20 ml. solution of 0.05 M initial concentration (C_0). The membranes had been washed repeatedly in distilled water to remove all soluble substances from them. The equilibration lasted for 150 hr. during which the flask was kept at constant temperature and shaken slightly. Actually, equilibrium appears to have been reached considerably sooner. For each set of measurements a blank was carried out simultaneously. This was prepared by equilibrating the membranes with distilled water. Use of a blank eliminated any error due to incomplete leaching. After equilibrium had been attained, about 3 ml. of solution was withdrawn from the flasks and analyzed.

Because concentrations had to be known with high accuracy, an automatic differential refractometer was used for the analyses. For greater details, refer to reference 13. The error in ΔC was estimated to be less than 0.5%. The distribution coefficient was then calculated in the following manner. By knowing the initial and eluent concentrations from the sorption experiments, one can determine the amount of solute absorbed in the membrane from the material balances:

$$V^s c^s + V^m c^m = V_i^s c_i^s \quad (29)$$

$$V_i^m = V^m \quad (30)$$

$$V_i^s = V^s \quad (31)$$

The subscript i indicates initial values. The quantity V_i^m was obtained by measuring the wet thickness and area of the membranes. Equations (30) and (31) were good approximations if the membranes were carefully surface dried. The other possible error, the volume changes caused by solute absorption, is well within the experimental error. From the solute content of the membrane the distribution coefficient was then obtained. The results are given in Table 1.

Membrane Thickness and Water Content

The wet thickness of the membranes was measured with a Light Wave Micrometer (Van Keuren Co., Watertown, Mass.). This type of micrometer utilizes an optical indication of pressure and can be read to one hundred thousandths of an inch. The compression of wet membranes, while measuring their thickness, caused some concern. For this reason, after the measurements were performed under 0.75 lb./sq. in. abs., further determinations were made under sequentially higher pressures up to 1.5 lb./sq. in. abs. No pressure effect was indicated by the results. It is possible, however, that a plateau has been reached at 0.75 lb./

TABLE 1. DISTRIBUTION COEFFICIENT AND VOLUME FRACTION OF WATER IN MEMBRANE

Solute	Initial conc.	Temp., °C.	Dist. coeff.	Volume fraction of water
Glucose	0.05 M	27	0.704	0.694
		37	0.695	0.689
		47	0.690	0.685
Sucrose	0.05 M	27	0.734	0.694
		37	0.721	0.689
		47	0.705	0.685
Raffinose	0.05 M	27	0.781	0.694
		37	0.760	0.685
		47	0.752	0.684

Membrane thickness: 0.00754 ± 0.00005 cm.

sq. in. abs. on a thickness-pressure diagram. To clarify this point, another set of thickness measurements was obtained by a Model PDR Carson-Dice Electronic Micrometer. The applied pressure of this instrument was only 1.9 g. The results agreed, within the experimental error, with that obtained by the Light Wave Micrometer.

The main problem in the determination of the water content of the membrane was to account for the droplets adhering to the surface of the membrane. Several methods were tried. First, an attempt was made to measure the rate of drying of the membrane. The next approach was to suspend the swollen membrane in a saturated water atmosphere and determine the water content from the dry and wet weights. However, none of these methods were successful. The technique finally adopted was to surface dry the membrane between filter papers after it was equilibrated in water. Then the membrane was weighed between two watch glasses and dried in an oven at 107°C . The water content was determined from the dry and wet weights and expressed as the fractional volume of cellophane made up of water. The density of the wet membrane was measured by a pycnometer. The procedure adopted is described in detail by Daniels et al. (3). The results are given in Table 1.

RESULTS

The thermodynamic description of intramembrane transport (in this investigation), assuming the Onsager reciprocal relation, has required three independent coefficients. The quantities directly measured were not always the phenomenological coefficients. From the experimental data the solute permeability coefficient at zero volume flow ω and the reflection coefficient σ were first calculated. The overall dialysis coefficient was defined by the equation

$$\frac{dN_s^I}{dt} = K_v A \Delta c_s \quad (32)$$

In terms of thermodynamic quantities, the rate of solute flow is (16)

$$\frac{1}{A} \frac{dN_s^I}{dt} = [\bar{c}_s L_p (1 - \sigma)] \Delta P + [\omega - \bar{c}_s L_p (1 - \sigma) \sigma] RT \Delta c_s \quad (33)$$

At $\Delta P = 0$

$$\frac{1}{A} \frac{dN_s^I}{dt} = [\omega - \bar{c}_s L_p (1 - \sigma) \sigma] RT \Delta c_s \quad (34)$$

Comparing (32) and (34)

$$\omega = \frac{K_v}{RT} + \bar{c}_s L_p (1 - \sigma) \sigma \quad (35)$$

In Equation (35), K_v is the overall dialysis coefficient and ω is the overall solute permeability coefficient at zero volume flow. These coefficients are characteristic of not only the membrane resistance R_m but also of the phase boundary resistances R_i 's:

$$R_v = \frac{1}{K_v} = R_m + R_1 + R_2 \quad (36)$$

The study of the phase boundary phenomena and the de-

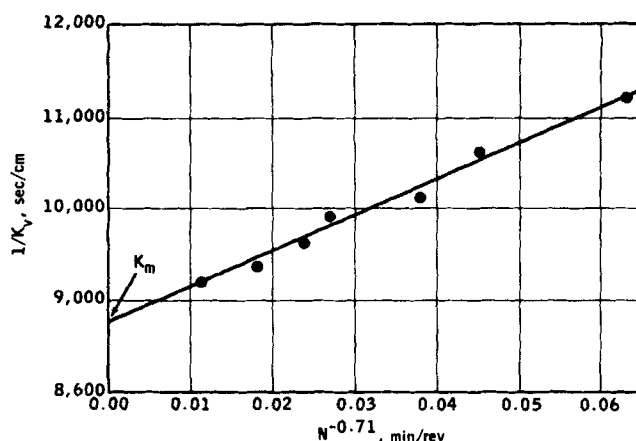


Fig. 3. Determination of overall dialysis coefficient.

termination of the mechanism of the phase boundary mass transport is described by the authors in a separate paper (14). Briefly, it was assumed that the phase boundary resistance, but not the membrane resistance, is a function of the fluid turbulence (and therefore also the stirrer speed) at the membrane-solution interface. When this function is known, it is possible to extend the solute transport results to a hypothetical infinite degree of turbulence, where the phase boundary resistances are entirely dissipated to obtain the resistance offered by the membrane alone. A typical plot of overall dialysis coefficient vs. stirrer speed is shown in Figure 3. From Equation (36) it follows, therefore, that when the turbulence $\rightarrow \infty$

$$\omega_m = \frac{K_m}{RT} + \bar{c}_s L_p (1 - \sigma) \sigma \quad (37)$$

This expression was used to calculate ω_m .

The reflection coefficient is defined as the ratio

$$\sigma = - \frac{L_{pD}}{L_p} \quad (38)$$

It has been earlier indicated that in measuring the cross-coefficient L_{pD} the phase boundary effects were found to be significant. No such observation was previously made in the literature. Actually, this effect is not surprising since the existing conditions at the phase boundary in these experiments are the same as in the solute permeability ones. The cross-coefficient which is only characteristic for the membrane alone was obtained through a similar analysis than the one used for K_v . The values of ω_m and σ are tabulated in Table 2. The phenomenological coefficient L_D was calculated from the relation

$$L_D = \frac{\omega_m}{\bar{c}_s} + L_p \sigma^2 \quad (39)$$

The elements of the matrix of phenomenological coefficients

$$\begin{bmatrix} L_p & L_{pD} \\ L_{pD} & L_D \end{bmatrix} \quad (40)$$

for the solutes glucose, sucrose, and raffinose are shown in Table 3. The second law of thermodynamics requires that the entropy production in an irreversible process must

TABLE 2. TABULATED VALUES OF ω_m AND σ

Solute	Temp., °C.	ω_m , moles/(atm.) (sq. cm.) (sec.)	σ , dimensionless
Glucose	27	4.56×10^{-9}	0.0885
	37	6.00	0.0791
	47	6.80	0.0711
Sucrose	27	2.85×10^{-9}	0.105
	37	3.64	0.0970
	47	4.24	0.0898
Raffinose	37	2.50×10^{-9}	0.126

TABLE 3. PHENOMENOLOGICAL COEFFICIENTS

Solute	Temp., °C.	L_D , cm./ (atm.) (sec.)	L_{Dp} , cm./ (atm.) (sec.)	L_p , cm./ (atm.) (sec.)	L_{pD} , cm./ (atm.) (sec.)
Glucose	27	1.19×10^{-4}	1.77×10^{-6}	2.00×10^{-5}	1.77×10^{-6}
	37	1.53	1.93	2.44	1.93
	47	1.73	2.17	3.05	2.17
Sucrose	27	7.49×10^{-5}	2.00×10^{-6}	1.90×10^{-5}	2.00×10^{-6}
	37	9.54	2.28	2.35	2.28
	47	10.96	2.72	3.03	2.72
Raffinose	37	6.56×10^{-5}	2.89×10^{-6}	2.30×10^{-5}	2.89×10^{-6}

always be positive. It can be shown (32) that this condition is satisfied if

$$4L_p L_D - (L_{pD} + L_{Dp})^2 \geq 0 \quad (41)$$

With Equation (9) this yields

$$L_p L_D - L_{pD}^2 \geq 0 \quad (42)$$

It is clear from Table 3 that this thermodynamic criterion is satisfied in all cases. These phenomenological coefficients give an unequivocal description of the transport process which takes place through the membrane.

FRICTIONAL COEFFICIENTS

In this investigation three sets of frictional coefficients were necessary to give a complete description of the membrane transport. These coefficients represent the different interactions between three entities: solute, solvent, and membrane. The magnitudes of the frictional coefficients were evaluated from Equations (15), (16), and (17) and presented in Table 4. Prior to calculating their values from the experimental data, the phase boundary contributions were eliminated from the rate constants. The values presented in Table 4 must be considered averages over the concentration differences that existed across the membrane in the experiments. Since these differences were relatively small, the frictional coefficients could be considered nearly constants in this range. As an approximation, the concentration gradients are assumed to be linear, and therefore the coefficients refer to a 0.05 molar solute concentration. The f_{ij} 's represent the frictional interaction between i and j per mole of i .

THE FRICTIONAL COEFFICIENTS f_{sw} AND f_{sm}

The frictional coefficient f_{sw} represents the interaction between one mole of solute and the water molecules in its vicinity inside the membrane. The magnitude of this term is indicative of the coincidence of solute and solvent path through the membrane. It is clear that when a solute is transported, for instance, by alignment of chemical bonds with the membrane matrix the value of f_{sw} should be close to zero. On the other hand, in a case of utmost idealization, where the membrane is compared to a bundle of straight capillary tubes acting mechanically, the magnitude of f_{sw} should be the same as in aqueous solution. Therefore, it should be interesting to evaluate this corresponding quantity in free solution and compare the two. In a dilute binary liquid system, the frictional coefficient between the two components is given by the relationship

$$f_{sw}^c = \frac{RT}{D} \quad (43)$$

where D is the binary diffusion coefficient.

Spiegler (29) suggested that the ratio f_{sw}^c/f_{sw} should be close to unity when allowance is made for the fact the volume concentration of free water in the solution is higher than in the resin. However, for the resin that he was studying the experimental ratio was found to be only 0.63. Mackay and Meares (20), also investigating ion exchange resins, speculated that these two terms should be different. The basic point of their argument was that when molecules pass through a membrane they have to follow a longer path than they would in traveling the same distance (that is, the membrane thickness) in free solution. Assuming a capillary model, the authors point out that this increased path length is due to the presence of water-filled channels which are not running perpendicular to the membrane surface. The ratio of membrane thickness to the actual distance is called the tortuosity factor. Finally, they conclude that the increased path length produces a proportionate increase in the frictional interaction between the two types of molecules when it is resolved in the direction of net flux. The authors showed that the tortuosity factor derived by the random walk treatment of diffusion through the aqueous phase of the membrane was in agreement with the ratio f_{sw}^c/f_{sw} . This term is given by

$$h = z^2/(2 - z)^2 \quad (44)$$

Equation (45a) implies that h is independent of the nature of solute and for a given solvent it only depends on the membrane characteristics.

It can be seen from Table 5 that for each system the magnitude of f_{sw} is considerably larger than that of f_{sw}^c . What is more important, this ratio increases with solute size, showing that Equation (44) does not apply to the present situation. The magnitudes of solute-membrane frictional coefficients f_{sm} indicate that for the carbohydrates used in this experiment the larger the solute size the stronger their interaction with the membrane matrix. These frictional coefficients refer to the interaction between one mole of solute and the macromolecular network in its vicinity. Due to these interactions the random motion of molecules is further increased which in turn lengthens the effective path. This is why the ratio f_{sw}^c/f_{sw} is the largest for glucose and smallest for raffinose. This related behavior can be expressed on a more quantitative basis. The definition of two reduced fric-

TABLE 4. FRICTIONAL COEFFICIENTS AS FUNCTION OF TEMPERATURE

Solute	Temp., °C.	f_{sw} , (atm.) (cm.) (sec.) / moles	f_{sm} , (atm.) (cm.) (sec.) / moles	f_{wm} , (atm.) (cm.) (sec.) / moles
Glucose	27	$1.79 \times 10^{+10}$	$2.47 \times 10^{+9}$	$8.18 \times 10^{+7}$
	37	$1.36 \times 10^{+10}$	$1.65 \times 10^{+9}$	$6.69 \times 10^{+7}$
	47	$1.21 \times 10^{+10}$	$1.38 \times 10^{+9}$	$5.34 \times 10^{+7}$
Sucrose	27	$2.78 \times 10^{+10}$	$6.08 \times 10^{+9}$	$8.43 \times 10^{+7}$
	37	$2.18 \times 10^{+10}$	$4.40 \times 10^{+9}$	$6.79 \times 10^{+7}$
	47	$1.89 \times 10^{+10}$	$3.03 \times 10^{+9}$	$5.27 \times 10^{+7}$
Raffinose	37	$3.06 \times 10^{+10}$	$9.82 \times 10^{+9}$	$6.63 \times 10^{+7}$

TABLE 5. THE RATIOS f_{sw}°/f_{sw} , AND f_{sw}/f_{sm}

Solute	Temp., °C.	f_{sw}°/f_{sw}	f_{sw}/f_{sm}
Glucose	27	0.194	7.24
	37	0.210	8.24
	47	0.194	8.75
Sucrose	27	0.164	4.60
	37	0.174	4.95
	47	0.171	6.22
Raffinose	37	0.156	3.11

tional coefficients

$$f_{sm}^* = [(f_{sm})_i / (f_{sm})_{\text{glucose}}]_T \quad (45)$$

$$f_{sw}^* = [(f_{sw}^{\circ}/f_{sw})_i / (f_{sw}^{\circ}/f_{sw})_{\text{glucose}}]_T \quad (46)$$

will facilitate the understanding of the basic relationships. Figure 4 shows a plot of f_{sw}^* vs. f_{sm}^* . An examination of this figure underlines the validity of the hypothesis that the ratio f_{sw}°/f_{sw} is related to intermolecular interaction between solute and membrane. Furthermore, a relation of this type can be used to estimate frictional coefficients with only a limited amount of data, that is, by using Equation (17) to calculate f_{sm} , and using Figure 4 to establish f_{sw} . This way only L_{pD} and L_p have to be determined for a given system. The only restriction is that the same solvent be used for each systems (constant f_{wm}).

COMPARISON OF FRICTIONAL COEFFICIENTS WITH DISTRIBUTION COEFFICIENTS

It is of particular interest to compare the characteristics of f_{sm} with those of the distribution coefficient K_D . It can be observed from Table 1 that K_D increases with the increasing molecular size of solute. This behavior can be explained by noting that hydrogen bonding and London forces are probably most responsible for the intermolecular attractions in the case of cellophane. Both of these forces favor local adsorption of the carbohydrates on the membrane matrix. The similarity of solute molecules to the polymer structure also enhances the interactions (9). These forces are stronger the larger the solute molecules (10) (for a homologous series), which explains the experimental findings that raffinose has a higher distribution coefficient than sucrose and in turn the value for sucrose is higher than for glucose. Similar interactions of a positive kind (as opposed to salting out effects) have been observed for ion exchange resins (23). The effect of temperature on distribution coefficient is a very complex phenomenon and little is known about it. The negative tem-

perature coefficient of hydrogen bonding might account for the decrease of K_D with increasing temperature noticed in this investigation.

The frictional data may now be examined in view of the above observations. The following points are apparent:

1. Just as the distribution coefficient, f_{sm} also increases with solute dimension. This relation is depicted in Figure 5.

2. The behavior of f_{sw}°/f_{sw} previously mentioned, that is, strong dependence on the nature of solute, agrees with the trends indicated by K_D .

It is clear that the transport of carbohydrates through the membrane is affected by the solute-membrane interactions. The solute permeability coefficient, when expressed in terms of frictional quantities, is given by the relationship

$$\omega_m = \frac{K_D}{\Delta x(f_{sm} + f_{sw})} \quad (47)$$

For the case of raffinose f_{sm} constitutes 25% of the total resistance. It is equally important, however, that the magnitude of f_{sw} is also indirectly influenced by the intermolecular forces between solute and membrane. The distribution coefficient which can be regarded as some, although by no means total, measure of these interactions exhibits a parallel behavior to f_{sm} .

WATER-MEMBRANE INTERACTION

The term f_{wm} is indicative of the frictional interaction between one mole of water molecules and the membrane matrix in its vicinity. As can be seen from Table 4 this quantity is smaller by two orders of magnitude than f_{sm} . This is not surprising in view of the high water content of cellophane. A considerable number of water molecules can remain quite distant from the macromolecular network of membrane and, therefore, there is little interaction between them and the polymer. The excellent agreement among the values of f_{wm} obtained in the three different systems (at the same temperature) gives some indication about the accuracy of the experiments. At 37°C., for instance, f_{sw} is $(6.70 \pm 0.06) \times 10^7$ (atm.)(cm.)(sec.)/moles.

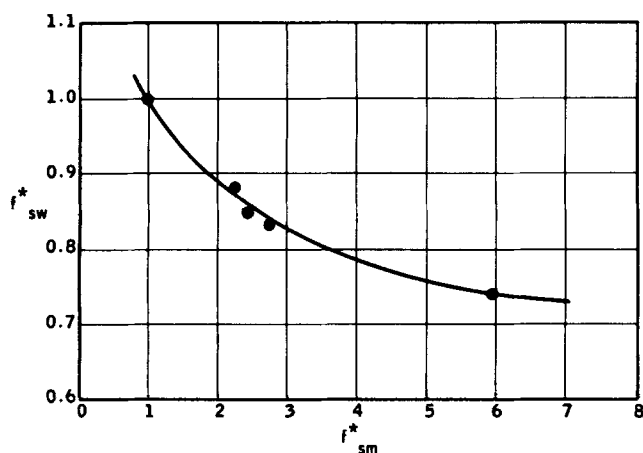


Fig. 4. The interdependence of the reduced frictional coefficients.

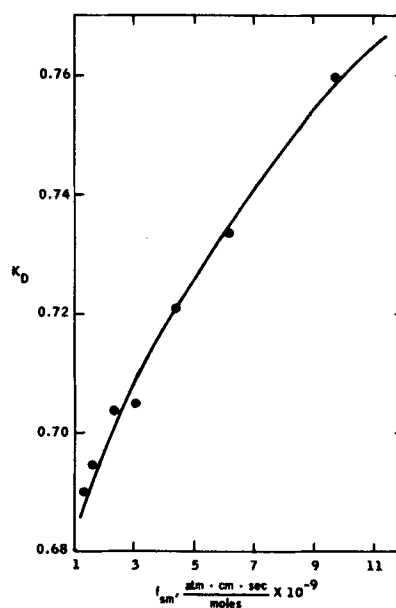


Fig. 5. Distribution coefficient vs. solute-membrane interaction.

SUMMARY

1. An equation which takes into account the movement of solvent across the membrane has been derived for the analysis of solute transport data. Errors up to 10% could have been introduced in this study by using the conventional equations but were avoided with the proposed one.

2. The phenomenological coefficients L_D , L_p , and L_{pD} which characterize the transport of glucose, sucrose, and raffinose through a cellophane membrane have been determined. The results were found to be thermodynamically consistent.

Phase boundary effects were significant in the determination of the cross-phenomenological coefficient L_{pD} . This investigation appears to be the first to study such effects.

The term L_p was found to be independent of the magnitude of applied pressure but strongly dependent on solute concentration.

The temperature dependence of the phenomenological coefficients was established.

3. The distribution coefficient was found to be different from the volume fraction of water in the membrane and a function of solute size.

4. The intramembrane transport mechanism has been investigated in terms of the frictional model. It was found that solute-polymer interactions were rather significant in determining solute permeation rates.

The solute-water interactions in the membrane were considerably larger than the corresponding quantities in aqueous solution. The difference between the two was related to the solute-membrane interactions and was expressed by the correlation between the reduced quantities f_{sm}^* and f_{sw}^* .

The concept of tortuosity factor was shown not to be a simple geometric characteristic of the membrane, but a quantity related to the collision frequency between solute and membrane matrix.

The distribution coefficient exhibited a parallel behavior to the solute-polymer interaction.

As expected, in view of the high water content of the membrane, water-membrane interactions were very small.

NOTATION

A = membrane area, sq. cm.
 c_i = concentration of species i , moles/cc.
 c_{av} = concentration in bulk stream, moles/cc.
 $c_{\text{sorberent}}$ = average concentration in membrane phase, moles/cc.
 C_i = concentration of species i in the membrane, moles/cc.
 D = molecular diffusion coefficient, sq. cm./sec.
 f_{ij} = frictional coefficient, (atm.)(cm.)(sec.)/moles
 f_{sw}^0 = frictional coefficient in free solution, (atm.)(cm.)(sec.)/moles
 F_{ij} = frictional force, (atm.)(sq. cm.)/moles
 h = tortuosity factor, dimensionless
 J_D = exchange flow, cm./sec.
 J_v = volume flow, cm./sec.
 K_D = distribution coefficient, dimensionless
 K_v = overall permeability coefficient, cm./sec.
 K_m = membrane permeability coefficient, cm./sec.
 L_D = phenomenological coefficient, cm./(atm.)(sec.)
 L_{Dp} = phenomenological coefficient, cm./(atm.)(sec.)
 L_{pD} = phenomenological coefficient, cm./(atm.)(sec.)
 L_p = phenomenological coefficient, cm./(atm.)(sec.)
 \dot{n}_i = transfer rate, moles/(sec.)(sq. cm.)
 P = pressure, atm.
 R_i = phase boundary resistance, sec./cm.
 R_m = membrane resistance, sec./cm.
 R_v = overall resistance, sec./cm.

T = temperature, °C.

v_i = velocity of species i in the membrane, cm./sec.

\bar{V}_i = partial molal volume of species i , cc./moles

V = volume, cc.

X_i = generalized thermodynamic force, (atm.)(sq. cm.)/moles

z = volume fraction of solution in membrane, dimensionless

ϕ_ω = water content of membrane, dimensionless

Δx = membrane thickness, cm.

ρ = density, moles/cc.

σ = reflection coefficient, dimensionless

ω = solute permeability coefficient, moles/(atm.)(sq. cm.)(sec.)

Subscripts

m = membrane

s = solute

w = water

Superscripts

I = compartment 1

II = compartment 2

LITERATURE CITED

1. Bjerrum, N., and E. Manegold, *Kolloid Z.*, **43**, 5 (1927).
2. Blunk, R. W., and S. Loeb, paper presented at AIChE Symp., College Park, Md. (1963).
3. Daniels, I. et al., "Experimental Physical Chemistry," McGraw-Hill, New York (1956).
4. DeGroot, S. R., "Thermodynamics of Irreversible Processes," North, Holland Publ., Amsterdam (1951).
5. Denbigh, K. G., "The Thermodynamics of Steady State," Wiley, New York (1951).
6. Ferry, J. D., *Chem. Rev.*, **18**, 373 (1936).
7. Fitts, D. D., "Nonequilibrium Thermodynamics," McGraw-Hill, New York (1962).
8. Ginzburg, B. Z., and A. Katchalsky, *J. Gen. Physiol.*, **47**, 403 (1963).
9. Helffrich, F., "Ion Exchange," McGraw-Hill, New York (1962).
10. Honeyman, J., "Recent Advances in the Chemistry of Cellulose and Starch," Heywood Co., London (1959).
11. Kahlenburg, A., *J. Phys. Chem.*, **10**, 141 (1908).
12. Katchalsky, A., *Proc. Symp. Transport Metabolism*, Prague (1961).
13. Kaufmann, T. G., Ph.D. dissertation, Columbia Univ., New York (1965).
14. ———, and E. F. Leonard, *AIChE J.*, in press.
15. Kedem, O., and A. Katchalsky, *Biochem. Biophys. Acta*, **27**, 229 (1959).
16. ———, *J. Gen. Physiol.*, **45**, 143 (1961).
17. ———, *Trans. Faraday Soc.*, **59**, 1918 (1963).
18. Kirkwood, J. G., in "Ion Transport Across Membranes," p. 119, Academic Press, New York (1954).
19. Lane, J. A., and J. W. Riggle, *Chem. Eng. Progr. Symp. Ser. No. 24*, **55**, 127 (1959).
20. Mackay, D., and P. Meares, *Trans. Faraday Soc.*, **55**, 1221 (1959).
21. Onsager, L., *Phys. Rev.*, **38**, 2265 (1931).
22. Pappenheimer, J. E., *Physiol. Rev.*, **33**, 387 (1953).
23. Reichenberg, D., and W. F. Wall, *J. Chem. Soc.*, 3364 (1956).
24. Reid, C. E., and E. J. Bretton, *J. Appl. Polymer Sci.*, **1**, 133 (1959).
25. Renkin, E. M., *J. Gen. Physiol.*, **38**, 225 (1954).
26. Schlögl, R., *Discussions Faraday Soc.*, **21**, 46 (1956).
27. Sliepcevich, G. M., and D. Finn, *Ind. Eng. Chem. Fundamentals*, **2**, 249 (1963).
28. Sourirajan, S., *ibid.*, **2**, 51 (1963).
29. Spiegler, K. S., *Trans. Faraday Soc.*, **54**, 1409 (1958).
30. Staverman, A. J., *Rec. Trav. Chem.*, **70**, 344 (1951).
31. ———, *Trans. Faraday Soc.*, **48**, 176 (1952).
32. Stewart, B. M., "Theory of Numbers," Macmillan, New York (1952).
33. Strutt, R. J. (Lord Rayleigh), *Proc. Math. Soc. (London)*, **4**, 36 (1873).
34. Vink, H., *Arkiv. Kemi.*, **19**, 15 (1961).
35. Weisner, H. B., *J. Phys. Chem.*, **34**, 335 (1930).

Manuscript received December 16, 1966; revision received April 24, 1967; paper accepted April 26, 1967. Paper presented at AIChE Detroit meeting.